Direct observation of controlled strain-induced second harmonic generation in a $Co_{0.25}Pd_{0.75}$ thin film on a $Pb(ZrTi)O_3$ substrate

Jae-Woo Jeong and Sung-Chul Shin
Department of Physics and Center for Nanospincs of Spinronic Materials, Korea Advanced Institute of Science and Technology, Taejon 305-701, Korea

N. N. Dadoenkova and I. L. Lyubchanskii
Donetsk Physical and Technical Institute of the National Academy of Sciences of Ukraine, 72, R. Luxemburg Str., 83114 Donetsk, Ukraine

V. K. Valev[a] and Th. Rasing[b]
Institute for Molecules and Materials, Radboud University Nijmegen, 6525 ED Nijmegen, The Netherlands

(Received 12 October 2006; accepted 19 December 2006; published online 23 January 2007)

The authors have observed strain-induced second harmonic generation (SHG) signals from a $Co_{0.25}Pd_{0.75}$ alloy film deposited on a lead zirconate titanate (PZT) substrate. The strain in the sample was controlled by the inverse piezoelectric effect. The authors demonstrate that it is possible to separate the strain contribution to the SHG signal from the crystallographic contribution and that from the electric polarization in PZT. An estimate of the value of the nonlinear photoelastic tensor components is in very good agreement with previous calculations. © *2007 American Institute of Physics*. [DOI: 10.1063/1.2433756]

Nonlinear optical effects like second harmonic generation (SHG) have been used to investigate bulk materials, surfaces, and interfaces, as the SHG signal is very sensitive to symmetry and structure changes such as caused by internal electric and magnetic fields, as well as crystallographic deformations such as strain.[1]

Strain-induced SHG in bulk materials and thin films was studied theoretically[2,3] and experimentally for various systems such as $Ba_{0.48}Sr_{0.52}TiO_3$ on a MgO(001) substrate,[4] $BaTiO_3$ and $Ba_xSr_{1-x}TiO_3$ thin films and $BaTiO_3/SrTiO_3$ superlattices,[5,6] semiconductor interfaces[7] and silicon wafers,[8,9] group III-nitride films, and thin Ag films on Si(111) substrates.[10,11] In most of these experimental papers strain was irreversibly induced by lattice mismatch between the film and the substrate,[4,8–11] whereas in Ref. 5 SHG was used for *in situ* detection of external stress. However, these studies were concerned only with the appearance of SHG or its enhancement. In order to get a direct evidence for strain-induced SHG, it is important that the signal is measured in a well-characterized system by a reliable method, i.e., with controllable and reproducible applied stress.

In this letter, we present results of a direct observation of strain-induced SHG in a $Co_{0.25}Pd_{0.75}$ alloy film deposited on a lead zirconate titanae (PZT) substrate. Using the inverse piezoelectric effect, the measurements were done under well-controlled and easily reproducible conditions. The thus obtained values of the nonlinear photoelastic (NPE) tensor components are in very good agreement with previous calculations.

A schematic diagram of the sample structure and of the measurement configuration is shown in Fig. 1. (For detailed sample preparation see Ref. 12.) The PZT film was deposited on a Pt(111) layer which in turn was deposited on a $Ti/SiO_2/Si$ substrate. It was fabricated by multiple spin coating of a PZT solution (Zr/Ti=52/48) (Ref. 12) and has a (111)-preferred orientation and a thickness of 1 μm. Subsequently, a 3 nm Pd film was deposited on the PZT substrate as a buffer layer and then a 3 nm $Co_{0.25}Pd_{0.75}$ alloy film was prepared and capped by a 3 nm Pd film. The piezoelectric coefficient d_{zzz} of the sample was about 270 pm/V, which is sufficient for the measurement of strain effects. The Pd and Pt layers were used as electrodes. In this vertical structure we can control the strain of the CoPd film on the PZT substrate with a low voltage and subsequently measure the effect of strain on the SHG signal.

The SHG measurements were performed using a Ti:sapphire laser at 800 nm with a pulse width of about 100 fs, a repetition rate of 82 MHz, and an average power of 50 mW. The incident beam went first through a Glan-Taylor polarizer and was then focused onto a spot of about 100 μm in diameter on the sample. The generated SHG signal (400 nm) was filtered by two BG360 color filters and, after going through the analyzer, was detected by a gated photon counter. For the

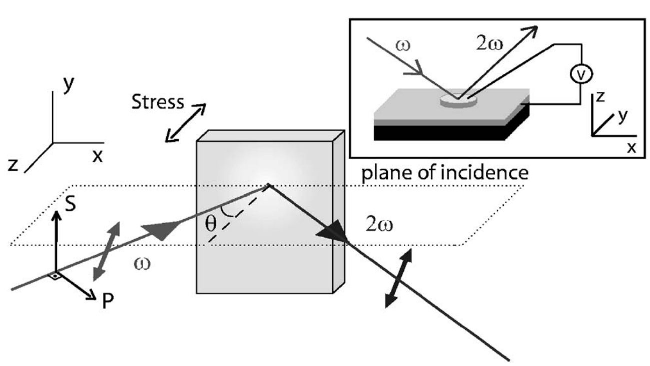

FIG. 1. Schematic diagram of the experiment. The voltage is applied along the z axis of the sample.

[a]Also at Institute for Nanoscale Physics and Chemistry (INPAC), Katholieke Universiteit Leuven, Celestijnenlaan 200 D, B-3001 Leuven, Belgium; electronic mail: v.k.valev@fys.kuleuven.be
[b]Electronic mail: th.rasing@science.ru.nl

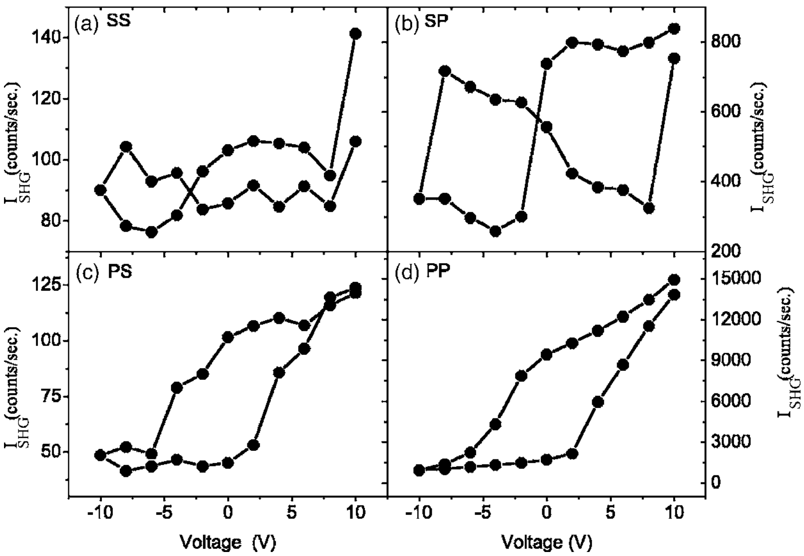

FIG. 2. SHG intensity as function of applied voltage for different polarizer-analyzer combinations.

fundamental and the second harmonic beam polarizations, both s- and p-polarized waves were studied.

In the dipole approximation the nonlinear optical polarization $\mathbf{P}^{\mathrm{NL}}(2\omega)$ at the double frequency ω of incident light can be written in the following form:[1]

$$\mathbf{P}_i^{\mathrm{NL}}(2\omega) = \chi_{ijk}^{(2)}(-2\omega{:}\omega,\omega)\mathbf{E}_j(\omega)\mathbf{E}_k(\omega), \quad (1)$$

where $\mathbf{E}(\omega)$ is the electric field of the incident light and $\chi_{ijk}^{(2)}$ is the second-order nonlinear optical susceptibility (NOS) tensor. The SHG intensity $I(2\omega)$, as function of the fundamental light intensity $I(\omega)$, is then given by $I(2\omega) \propto |P^{\mathrm{NL}}(2\omega)|^2 \propto |\chi_{ijk}^{(2)}|^2 I^2(\omega)$.

In the limit of ultrathin films, we consider an averaged interface contribution $\tilde{\chi}_{ijk}^{(2)}$ from all the interfaces in the $Pd/Co_{0.25}Pd_{0.75}/Pd$ trilayer. In the following, we will omit the tilde sign.

There are several possible contributions to the $\mathbf{P}^{\mathrm{NL}}(2\omega)$, which are responsible for the SHG. First of all, we must consider the crystallographic terms that depend on the symmetry of the present system.[1] Next, there is the contribution from the electric polarization $\mathcal{P}$ of the ferroelectric substrate,

$$\mathcal{P}_i = \mathcal{P}_i^{(0)} + \kappa_{ij} E_j^{\mathrm{int}}, \quad (2)$$

where $\mathcal{P}^{(0)}$ is the spontaneous polarization of the ferroelectric substrate, κ_{ij} is the dielectric sucseptibility, and $\mathbf{E}^{\mathrm{int}}$ is the internal electric field. Because of the inverse piezoelectric effect, the applied electric field in the PZT leads to the appearance of strain,[13]

$$u_{ij} = d_{ijk} E_k^{\mathrm{int}}, \quad (3)$$

where u_{ij} is the strain tensor and d_{ijk} is the tensor describing the inverse piezoelectric effect. This strain contributes to $\mathbf{P}^{\mathrm{NL}}(2\omega)$ due to the NPE effect.[14] Because we did not observe any magnetic contrast in our measurements, possible magnetic contributions to the SHG (Ref. 15) can be ignored.

All these contributions can be represented in the following form:[2,3]

$$\chi_{ijk}^{(2)} = \chi_{ijk}^{(2,0)} + p_{ijklm} u_{lm} + \chi_{ijkl}^{(3,0)} \mathcal{P}_l, \quad (4)$$

where $\chi_{ijk}^{(2,0)}$ is the purely electronic NOS tensor, p_{ijklm} is the NPE tensor, and $\chi_{ijkl}^{(3,0)}$ is the third-order NOS tensor, which is responsible for the electric-field-induced contribution.[1]

As shown in Fig. 1, the electric field was applied along the z axis, causing an electric polarization along the same direction in the (111)-oriented PZT substrate. This electric field generates strain characterized by the u_{xx}, u_{yy}, and u_{zz} components of the strain tensor. Taking into account the nonzero components of the $\chi_{ijk}^{(2,0)}$, p_{ijklm}, and $\chi_{ijkl}^{(3,0)}$ tensors for the C_{3v} symmetry group,[16] which characterizes the interface between the film and the substrate, we can find the contributions of all mechanisms to SHG in the above-mentioned geometries of our experiment,

$$\begin{pmatrix} \mathbf{P}_S^{\mathrm{NL}}(2\omega) \\ \mathbf{P}_P^{\mathrm{NL}}(2\omega) \end{pmatrix} = \begin{pmatrix} \chi_{s;ss}^{(\mathrm{eff})} & \chi_{s;pp}^{(\mathrm{eff})} \\ \chi_{p;ss}^{(\mathrm{eff})} & \chi_{p;pp}^{(\mathrm{eff})} \end{pmatrix} \begin{pmatrix} E_s^2(\omega) \\ E_p^2(\omega) \end{pmatrix}, \quad (5)$$

$$\chi_{s;ss}^{(\mathrm{eff})} = \chi_{yyy}^{(2,0)},$$

$$\chi_{p;ss}^{(\mathrm{eff})} = \{(\chi_{xyyz}^{(3,0)}\mathcal{P}_z + p_{xyyzz}u_{zz})^2 + (\chi_{zyy}^{(2,0)} + \chi_{zyyz}^{(3,0)}\mathcal{P}_z + p_{zyyxx}u_{xx} + p_{zyyyy}u_{yy} + p_{zyyzz}u_{zz})^2\}^{1/2},$$

$$\chi_{s;pp}^{(\mathrm{eff})} = \chi_{yxx}^{(2,0)} \cos^2\theta,$$

$$\begin{aligned}\chi_{p;pp}^{(\mathrm{eff})} = \{&[(\chi_{xxxz}^{(3,0)}\mathcal{P}_z + p_{xxxxx}u_{xx} + p_{xxxyy}u_{yy} + p_{xxxzz}u_{zz})\cos^2\theta \\ &+ (\chi_{xzx}^{(2,0)} + \chi_{xxz}^{(2,0)} + \chi_{xxzz}^{(3,0)}\mathcal{P}_z + 2p_{xzxxx}u_{xx} + 2p_{xzxyy}u_{yy} \\ &+ 2p_{xzxzz}u_{zz})\cos\theta\sin\theta + (p_{xzzxx}u_{xx} \\ &+ p_{xzzyy}u_{yy})\sin^2\theta]^2 + [(\chi_{zxx}^{(2,0)} + \chi_{zxxz}^{(3,0)}\mathcal{P}_z + p_{zxxxx}u_{xx} \\ &+ p_{zxxyy}u_{yy} + p_{zxxzz}u_{zz})\cos^2\theta + (\chi_{zzz}^{(2,0)} \\ &+ p_{zzzzz}u_{zz})\sin^2\theta]^2\}^{1/2}, \end{aligned} \quad (6)$$

where $\mathbf{P}_S^{\mathrm{NL}}(2\omega)$ and $\mathbf{P}_P^{\mathrm{NL}}(2\omega)$ correspond to the S_{out} and P_{out} components of the $\mathbf{P}^{\mathrm{NL}}(2\omega)$, ss and pp indicate the input polarization (i.e., correspond to s_{in} and p_{in}), and θ is the angle of incidence. From Eqs. (5) and (6) it follows that the $s_{\mathrm{in}} \to S_{\mathrm{out}}$ and $p_{\mathrm{in}} \to S_{\mathrm{out}}$ signals are induced by the components of the second-order NOS tensor $\chi_{ijk}^{(2,0)}$, whereas for the $s_{\mathrm{in}} \to P_{\mathrm{out}}$ and $p_{\mathrm{in}} \to P_{\mathrm{out}}$ signals all tensors from Eq. (4) contribute to the SHG.

Figure 2 shows the experimental results for all four geometries: $s_{\mathrm{in}} \to S_{\mathrm{out}}$, $s_{\mathrm{in}} \to P_{\mathrm{out}}$, $p_{\mathrm{in}} \to S_{\mathrm{out}}$, and $p_{\mathrm{in}} \to P_{\mathrm{out}}$. The applied voltage was first swept from +10 to −10 V and then back to +10 V. The corresponding hysteresis curves are af-

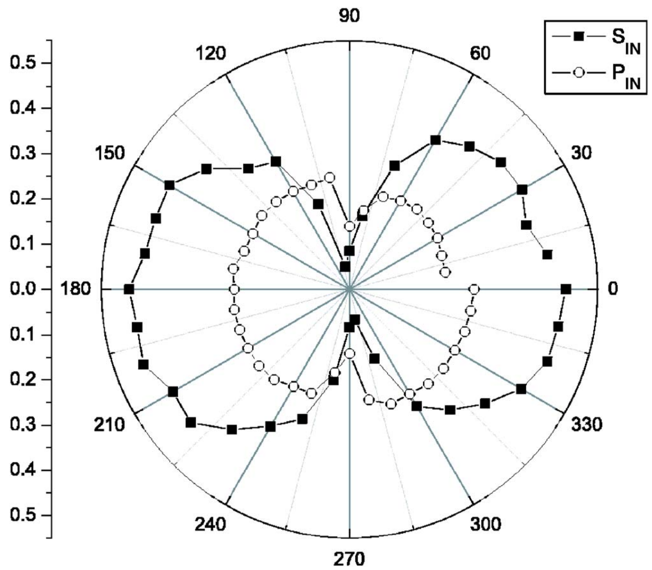

FIG. 3. Strain-induced asymmetry of SHG for for s_{in}- and p_{in}-polarized incident light. The 0° for the analyzer rotation corresponds to the P_{out} direction.

fected differently by the various contributing tensors. In accordance with Eqs. (5) and (6), the most intensive SHG signal was observed for $p_{in} \rightarrow P_{out}$, whereas for $s_{in} \rightarrow P_{out}$ the signal was much weaker. For the remaining geometries it was even less, approximately by two orders of magnitude. The high value of the SHG intensity in the $p_{in} \rightarrow P_{out}$ geometry is due to the large value of $\chi^{(2,0)}_{zzz}$.[17] The significantly smaller SHG signals for $s_{in} \rightarrow S_{out}$ and $p_{in} \rightarrow S_{out}$ geometries can be explained by the small values of $\chi^{(2,0)}_{yyy}$ and $\chi^{(2,0)}_{yxx}$, together with a contribution from the misfit strain between the $Pd/Co_{0.25}Pd_{0.75}/Pd$ trilayer and the substrate.[2] Here, at the coercivity voltage $U_c = \pm 3$ V, the contribution to the SHG signal from the electric polarization $\mathcal{P}$ equals zero.[12] As a result, only the nonzero components of the second-order NOS and of the NPE tensors contribute to the SHG signal for this situation. Because the sign of the u_{xx}, u_{yy}, and u_{zz} components of the strain tensor depends on the direction of the internal electric field [Eq. (3)], we can compare the SHG intensities for the two opposite directions of $\mathbf{E}^{int}$: "up" $I^{\uparrow}(2\omega)$ and "down" $I^{\downarrow}(2\omega)$. We can then obtain the asymmetry A_{SHG} of the strain-induced SHG,

$$A_{SHG} = \frac{I^{\uparrow}(2\omega) - I^{\downarrow}(2\omega)}{I^{\uparrow}(2\omega) + I^{\downarrow}(2\omega)}. \quad (7)$$

The angular dependence of A_{SHG} is presented in Fig. 3, where the analyzer was rotated from an initial position along P, for s_{in}- and p_{in}-polarized incident light. In good agreement with Eqs. (5) and (6), the A_{SHG} curves are oriented along the P_{out} direction.

From the measured values of A_{SHG} we can estimate the effective values of the NPE tensor components. Assuming that the second-order NOS tensor components are dominant with respect to the NPE terms, we can rewrite Eq. (7) as

$$A_{SHG} \propto \frac{|p^{NL,eff} d_{zzz} E^{int}_z|}{|\chi^{(2,0)}|} \cos \varphi, \quad (8)$$

where φ is the phase between the crystallographic and NPE contributions and $p^{NL,eff}$ is the effective value of the nonzero NPE tensor components. The strength of the internal electric field is determined by $E^{int}_z = U/t_f$, where U is the applied external voltage and t_f is the total thickness of the film. For $\varphi \approx 0$, substituting the numerical values into Eq. (8), we obtain

$$p^{NL,eff}_{s\rightarrow P} \approx 6 \times 10^2 \cdot \chi^{(2,0)}_{s;pp},$$

$$p^{NL,eff}_{p\rightarrow P} \approx 3 \times 10^2 \cdot \chi^{(2,0)}_{p;pp}. \quad (9)$$

It should be noted that these estimations are in very good agreement with our previous calculations of the NPE tensor components for $Y_3Fe_5O_{12}$ [see Eq. (21) in Ref. 18].

In conclusion, we have measured strain-induced SHG in $Pd/Co_{0.25}Pd_{0.75}/Pd$ thin film deposited on a PZT substrate using the inverse piezoelectric effect in well-controlled and reproducible way via the inverse piezoelectric effect. By selecting the appropriate applied voltage and polarizer-analyzer combination, we were able to separate the strain-induced SHG from the crystallographic and the electric polarization contributions to the SHG signal. Finally, based on the measurements of the voltage controlled asymmetry A_{SHG} of this strain-induced signal, we made an estimate of the nonlinear photoelastic tensor components, which is in very good agreement with our previous calculations.

The authors would like to thank J.-W. Lee for sample preparation. J.-W.J. and I.L.L. are grateful to the IMM at the Radboud University Nijmegen for the hospitality during their staying in Nijmegen. This work was supported in part by the KOSEF, the EU project DYNAMICS, the Dutch NanoNed program, FOM, and INTAS, Grant No. 03-51-3784.

[1] Y. R. Shen, *The Principles of Nonlinear Optics* (Wiley, New York, 1984).
[2] I. L. Lyubchanskii, N. N. Dadoenkova, M. I. Lyubchanskii, Th. Rasing, J.-W. Jeong, and S.-C. Shin, Appl. Phys. Lett. **76**, 1848 (2000).
[3] J.-W. Jeong, S.-C. Shin, I. L. Lyubchanskii, and V. N. Varyukhin, Phys. Rev. B **62**, 13455 (2000).
[4] U. C. Oh, J. Ma, G. K. L. Wong, J. B. Ketterson, and J. H. Je, Appl. Phys. Lett. **76**, 1461 (2000).
[5] T. Zhao, H. Lu, F. Chen, G. Yang, and Z. Chen, J. Appl. Phys. **87**, 7448 (2000).
[6] I. I. Smolyaninov, H. Y. Liang, C. H. Lee, and C. C. Davis, J. Appl. Phys. **89**, 206 (2001).
[7] G. Lüpke, Surf. Sci. Rep. **35**, 75 (1999).
[8] J. Reif, R. Schmid, Th. Shneider, and D. Wolgfframm, Solid-State Electron. **44**, 809 (2000).
[9] G. Lucovsky and J. C. Phillips, Appl. Phys. A **78**, 453 (2004).
[10] C.-S. Chen, J.-T. Lue, C.-L. Wu, S. Gwo, and K.-Y. Lo, J. Phys.: Condens. Matter **15**, 6537 (2003).
[11] C.-S. Chen and J.-T. Lue, Eur. Phys. J. B **46**, 367 (2005).
[12] J.-W. Lee, S.-C. Shin, and S.-K. Kim, Appl. Phys. Lett. **82**, 2458 (2003).
[13] B. A. Strukov and A. P. Levanyuk, *Ferroelectric Phenomena in Crystals: Physical Foundations* (Springer, Berlin, 1998).
[14] D. F. Nelson and M. Lax, Phys. Rev. B **3**, 2795 (1971).
[15] A. Kirilyuk and Th. Rasing, J. Opt. Soc. Am. B **22**, 148 (2005).
[16] R. R. Birss, *Symmetry and Magnetism*, Series of Monographs on Selected Topics in Solid State Physics, 2nd ed. (North-Holland, Amsterdam, 1966).
[17] W. Hübner, K. H. Bennemann, and K. Böhmer, Phys. Rev. B **50**, 17597 (1994).
[18] I. L. Lyubchanskii, N. N. Dadoenkova, M. I. Lyubchanskii, Th. Rasing, J.-W. Jeong, and S.-C. Shin, J. Appl. Phys. **87**, 6794 (2000).